

Gene-modified pig-to-human liver xenotransplantation


<https://doi.org/10.1038/s41586-025-08799-1>

Received: 5 June 2024

Accepted: 18 February 2025

Published online: 26 March 2025

Open access

 Check for updates

Kai-Shan Tao^{1,16}, Zhao-Xu Yang^{1,16}, Xuan Zhang^{1,16}, Hong-Tao Zhang^{1,16}, Shu-Qiang Yue¹, Yan-Ling Yang¹, Wen-Jie Song¹, De-Sheng Wang¹, Zheng-Cai Liu¹, Hai-Min Li¹, Yong Chen¹, Rui Ding¹, Shi-Ren Sun², Ming Yu³, Ji-Peng Li⁴, Wei-Xun Duan⁵, Zhe Wang⁶, Jing-Wen Wang⁷, Jia-Yun Liu⁸, Min-Wen Zheng⁹, Xi-Jing Zhang^{10,11}, Wen Yin¹², Wei-Jun Qin¹³, Dong-Mei Bian¹⁴, Lin Li¹, Min Li¹, Zhi-Bin Lin¹, Hao Xu¹, Dan Wei¹, Hong Zhang¹, Juan-Li Duan¹, Deng-Ke Pan¹⁵, Hai-Long Dong^{11✉}, Lin Wang^{1✉} & Ke-Feng Dou^{1✉}

The shortage of donors is a major challenge for transplantation; however, organs from genetically modified pigs can serve as ideal supplements^{1,2}. Until now, porcine hearts and kidneys have been successively transplanted into humans^{3–7}. In this study, heterotopic auxiliary transplantation was used to donate a six-gene-edited pig liver to a brain-dead recipient. The graft function, haemodynamics, and immune and inflammatory responses of the recipient were monitored over the subsequent 10 days. Two hours after portal vein reperfusion of the xenograft, goldish bile was produced, increasing to 66.5 ml by postoperative day 10. Porcine liver-derived albumin also increased after surgery. Alanine aminotransferase levels remained in the normal range, while aspartate aminotransferase levels increased on postoperative day 1 and then rapidly declined. Blood flow velocity in the porcine hepatic artery and portal and hepatic veins remained at an acceptable level. Although platelet numbers decreased early after surgery, they ultimately returned to normal levels. Histological analyses showed that the porcine liver regenerated capably with no signs of rejection. T cell activity was inhibited by anti-thymocyte globulin administration, and B cell activation increased 3 days after surgery and was then inhibited by rituximab. There were no significant peri-operative changes in immunoglobulin G or immunoglobulin M levels. C-reactive protein and procalcitonin levels were initially elevated and then quickly declined. The xenograft remained functional until study completion.

Liver transplantation is the most effective treatment for end-stage liver diseases. However, the number of allogeneic donations fails to meet the growing demand for transplants. To address the shortage, porcine organs are being considered as an ideal supplement given their compatible physiological function and size^{1,2}. Moreover, theoretical and technical advances in gene editing have enabled the removal of key genes that mediate hyperacute rejection, such as glycoprotein α -galactosyltransferase 1 (GGTA1) and cytidine monophosphate-*N*-acetylneuraminic acid hydroxylase (CMAH), and the insertion of human transgenes that facilitate xenograft compatibility, including thrombomodulin and haem-oxygenase 1 (refs. 8–11).

Several preclinical and clinical xenotransplantation studies have been performed so far. Porcine hearts and kidneys have been

successfully transplanted into both living and brain-dead individuals^{3–7}. A recent study externally attached a pig liver to a brain-dead person with liver failure and assessed liver function, serving as the first use of pig liver to treat a human disease¹². However, because of the complexity of liver function, to our knowledge no liver xenotransplantation has been performed in a living person before this trial.

Our team has conducted liver xenotransplantation research for more than a decade^{13–15}. In 2013, we successfully performed the first pig-to-monkey heterotopic auxiliary liver transplantation in China. Both the recipient monkey and the transplanted liver survived for 14 days¹⁶. Since then, we have conducted, alone or in collaboration with other groups, pig-to-monkey liver, heart, kidney, cornea, skin and bone xenotransplantation, and a single pig-to-human skin xenotransplantation. In this study, under the strict supervision of our hospital

¹Department of Hepatobiliary Surgery, Xijing Hospital, Fourth Military Medical University, Xi'an, China. ²Department of Nephrology, Xijing Hospital, Fourth Military Medical University, Xi'an, China. ³Department of Ultrasound, Xijing Hospital, Fourth Military Medical University, Xi'an, China. ⁴Department of Experimental Surgery, Xijing Hospital, Fourth Military Medical University, Xi'an, China. ⁵Department of Cardiovascular Surgery, Xijing Hospital, Fourth Military Medical University, Xi'an, China. ⁶Department of Pathology, Xijing Hospital, Fourth Military Medical University, Xi'an, China. ⁷Department of Pharmacy, Xijing Hospital, Fourth Military Medical University, Xi'an, China. ⁸Department of Clinical Laboratory Medicine, Xijing Hospital, Fourth Military Medical University, Xi'an, China. ⁹Department of Radiology, Xijing Hospital, Fourth Military Medical University, Xi'an, China. ¹⁰Department of Critical Care Medicine, Xijing Hospital, Fourth Military Medical University, Xi'an, China. ¹¹Department of Anesthesiology and Perioperative Medicine, Xijing Hospital, Fourth Military Medical University, Xi'an, China. ¹²Department of Transfusion Medicine, Xijing Hospital, Fourth Military Medical University, Xi'an, China. ¹³Department of Urology, Xijing Hospital, Fourth Military Medical University, Xi'an, China. ¹⁴Department of Surgery Operating Room, Xijing Hospital, Fourth Military Medical University, Xi'an, China. ¹⁵Chengdu Clonorgan Biotechnology Co. Ltd, Chengdu, China. ¹⁶These authors contributed equally: Kai-Shan Tao, Zhao-Xu Yang, Xuan Zhang, Hong-Tao Zhang. ✉e-mail: hldong6@hotmail.com; fierywang@163.com; doukef@fmmu.edu.cn

Article

ethics committee, we xenotransplanted the liver from a six-gene-edited pig to a brain-dead person¹⁷.

Evaluation of the gene-modified pig

A six-gene-modified Bama miniature pig kindly provided by Clonorgan Biotechnology was used as the donor in this study (Fig. 1a). To confirm the success of the gene modification, flow cytometry was performed on peripheral blood mononuclear cells (PBMCs) collected from the donor pig. *GGTA1* (synthesizing α -1,3-galactosyltransferase), *B4GALNT2* (encoding β -1,4-*N*-acetyl-galactosaminyltransferase 2) and *CMAH* (synthesizing *N*-glycolylneuraminic acid (Neu5Gc)), which mediates hyperacute rejection, were largely inactivated in the pig (Fig. 1b). Meanwhile, flow cytometry and western blotting showed that human complement regulatory proteins (CRPs), including CD46 (membrane cofactor protein) and CD55 (decay-accelerating factor), which attenuate hyperacute rejection and prolong xenograft survival, were overexpressed in donor PBMCs (Fig. 1b,c). To activate antithrombotic protein C and prevent clot formation, human thrombomodulin (*THBD*, encoding hTBM) was inserted into the porcine genome. Immunohistochemistry staining (IHC) showed that hTBM, as well as CD46 and CD45, were upregulated following gene modification (Fig. 1d). The recipient was confirmed to have low levels of xenoreactive immunoglobulin M (IgM) and IgG antibodies by flow cytometry (Fig. 1e,f). Porcine endogenous retrovirus (PERV) attached to the donor pig could not be detected peri-operatively in the recipient's PBMCs or liver (Fig. 1g and Extended Data Fig. 1b), and porcine cytomegalovirus (PCMV) was also diminished in the donor and the recipient's liver (Fig. 1h and Extended Data Fig. 1a). Moreover, microchimerism was undetectable in the recipient (Extended Data Fig. 1b).

Heterotopic auxiliary liver transplant

Before transplantation, vascular segmentation was performed (Extended Data Fig. 3a,b) on the donor pig, and the sizes of the porcine portal vein (PV) and inferior vena cava (IVC) were shown to approximately match the recipient's vessels (Extended Data Fig. 2a). Photographs of a ruddy porcine liver captured at different time points are shown in Extended Data Fig. 2b. On the basis of our experience of earlier liver transplants, we chose to perform a heterotopic auxiliary transplantation. In brief, the recipient's IVC was partially removed below the level of the right renal vein. The supra-hepatic IVC of the donor liver was then connected to the proximal end of the recipient's IVC (Extended Data Fig. 2c and Ⓞ in Extended Data Fig. 2d) and the porcine PV was anastomosed with the distal end of the recipient's IVC (Extended Data Fig. 2c and ⊙ in Extended Data Fig. 2d). The porcine hepatic artery was then bridged to the recipient's abdominal aorta (Extended Data Fig. 2c and ⊙ in Extended Data Fig. 2d) and the bile was drained from the body (Extended Data Figs. 2d and 3c). At the end of the study, the porcine liver was removed and the recipient's IVC was reconstructed using an artificial blood vessel (Extended Data Fig. 3d,e).

The porcine liver remained functional

To assess the function of the transplanted liver, an explicit schedule for further analyses was established (Fig. 2a). Goldish bile produced by the porcine liver emerged 2 h after PV reperfusion and increased markedly postoperatively (Fig. 2b,c). Porcine liver-derived albumin detected by enzyme-linked immunosorbent assay was also augmented following surgery (Fig. 2d). Even if the amounts of pig-originated bile and albumin had been low, these findings indicated the liver could survive in a human body and start functioning. Notably, there were inconsistent changes in the levels of alanine aminotransferase (ALT) and aspartate aminotransferase (AST), the enzymes that reflect liver function, following transplantation. Although ALT amounts remained

normal, AST amounts increased sharply shortly after surgery and then declined rapidly (Fig. 2e,f). Although the reason for this discrepancy remains unclear, the marked increase in AST is unlikely to imply graft malfunction. Meanwhile, other indicators of liver function were measured (Fig. 2g–k). The amount of alkaline phosphatase was maintained in the normal range throughout the study (Fig. 2k), whereas bilirubin and γ -glutamyl transpeptidase (γ -GGT) were elevated at the late stage of the study (Fig. 2g–j).

Haemodynamics following transplantation

To confirm successful re-establishment of the porcine vascular system, blood flow in the porcine hepatic artery, PV and hepatic vein was monitored continuously by ultrasound. Blood flow in the porcine hepatic artery remained in the high-speed category following surgery, ranging from 41.45 to 60.63 cm s⁻¹; the velocity of blood flow in the PV and hepatic vein was also acceptable (Extended Data Fig. 4a,b). Portal vein flow (PVF) was stable throughout the study (Extended Data Fig. 4c). Because some preclinical trials have reported impairments in coagulation function after xenografting, the recipient's coagulation status was evaluated. Unlike prothrombin time (PT), which was sustained in the physiological range, a decrease in platelets (PLT) and an increase in activated partial thromboplastin time (APTT) were observed during the early stage of the postoperative period; however, both ultimately recovered to normal levels (Fig. 2l–n). These data indicate that intrinsic coagulation was more affected by the xenograft than extrinsic coagulation and that the hTBM transgene efficiently maintained circulatory homeostasis (Extended Data Fig. 5a,b).

Histological analyses of porcine liver

Histological changes to the donor liver were next assessed using haematoxylin and eosin, IHC and immunofluorescent staining, scanning electron microscopy (SEM) and transmission electron microscopy (TEM). Surprisingly, slight sinusoidal congestion and inflammatory cell infiltration were found peri-operatively in the porcine liver, but no signs of immune rejection were noted. Moreover, the recipient's original liver tissue collected on day 10 exhibited mild intrahepatic cholestasis (Fig. 3a), which may account for the elevated bilirubin and γ -GGT amounts observed during the late stage of the investigation (Fig. 2g–j). The histology of the hepatocytes, stellate cells and liver sinusoidal endothelial cells (LSECs) in the transplanted liver was also assessed. The porcine liver collected on day 10 had higher hepatocyte proliferation (Ki67), lower stellate cell activation (alpha smooth muscle actin) and higher LSEC repopulation (CD31) than the pre-operative control (Fig. 3b). These findings indicated that the transplanted liver capably regenerated with no sign of rejection and fibrogenesis. Interestingly, LSECs observed by SEM possessed well-differentiated fenestrae, indicating that the microcirculation of the porcine liver was not disrupted following transplantation (Fig. 3b). Ultimately, TEM observation showed that there was no big difference in the ultrastructure of the porcine hepatocytes between the 0 day and 10 day groups, and no viral particles were observed (Fig. 3c).

The xenograft-triggered immune response

An excessive immune response induced by xenotransplantation is the leading reason for xenograft dysfunction. All the drugs used for immunosuppression are listed in Extended Data Fig. 6. In brief, methylprednisolone, tacrolimus and mycophenolate mofetil, which are commonly used immunosuppressants, were administered during the postoperative period. Etanercept and rituximab, which trigger anti-tumour necrosis factor (TNF) responses and B lymphocyte resolution, respectively, were also used intermittently following surgery. Anti-thymocyte globulin and eculizumab were used only pre-operatively. The blood

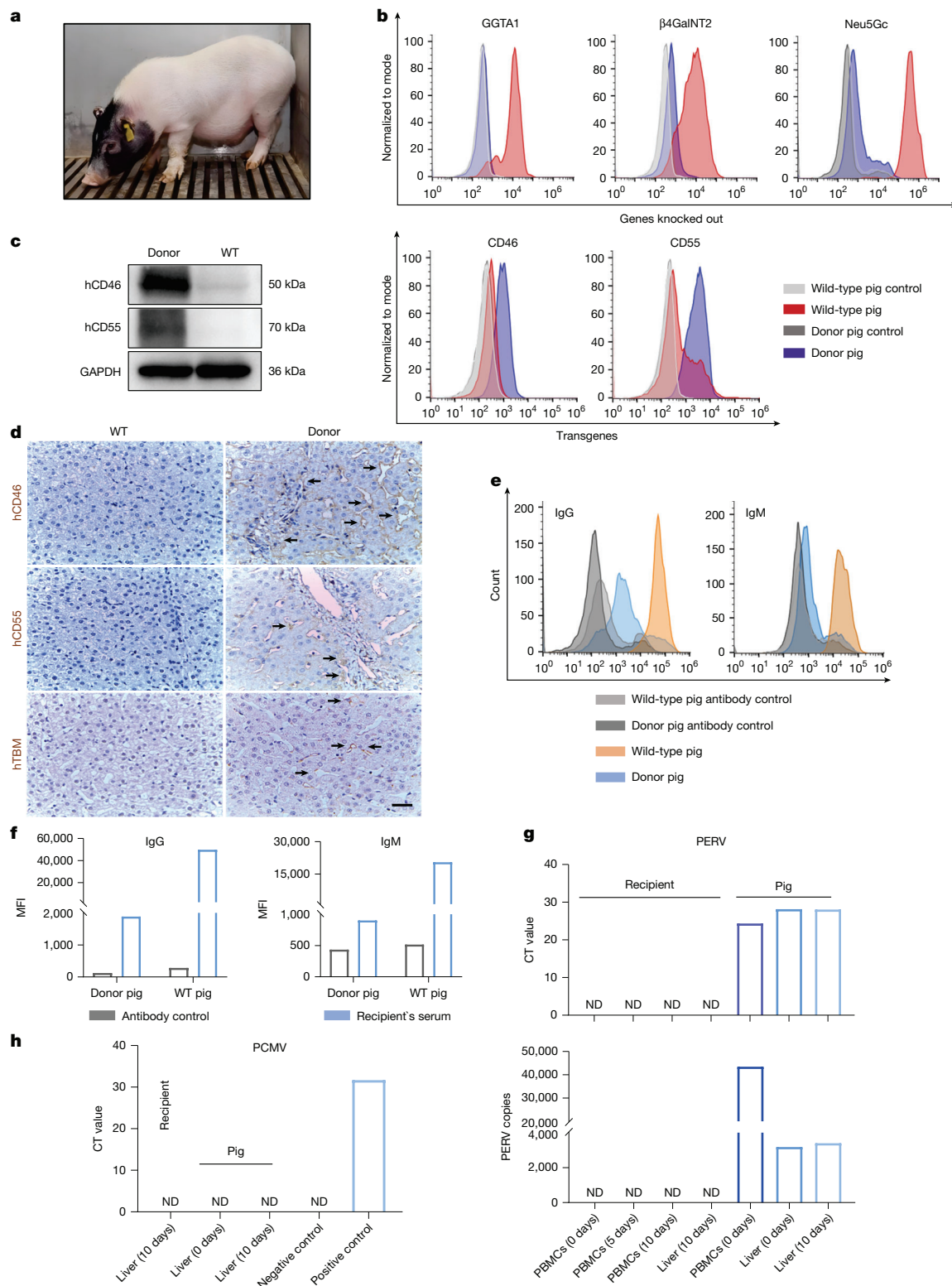


Fig. 1 | Gene editing and pathogenic surveillance of the donor pig. **a**, Donor pig. **b**, Flow cytometry result showing the numbers of GGT1-, β 4GalNT2-, Neu5Gc-, CD46- and CD55-positive cells in the donor pig and a wild-type (WT) pig. For gating strategies, see Supplementary Fig. 3. **c**, Western blotting result showing the levels of human CD46 and CD55 protein in the liver tissues of the donor and a wild-type pig. Glyceraldehyde 3-phosphate dehydrogenase (GAPDH) is used as the control. For blot source data, see Supplementary Fig. 1. **d**, IHC staining result showing the levels of human CD46, CD55 and thrombomodulin protein in the liver tissues of the donor and a wild-type pig. Positive signals are represented by black arrows. **e**, Flow cytometry result showing the ability of

PBMCs, isolated from the donor and the wild-type pig, to bind human IgM and IgG, represented by median fluorescence intensity (MFI). For gating strategies, see Supplementary Fig. 3. **f**, Quantitative result of **e**. **g**, Relative (upper) and absolute (lower) quantification of real-time polymerase chain reaction (RT-PCR) showing the number of PERV copies in the PBMCs and liver tissues of the recipient and the donor pig. **h**, Relative quantification of RT-PCR showing PCMV quantity in the liver tissues of the recipient and the donor pig. **b–h** contain one biological and technical repetition. Two independent experiments were carried out in **c** and **d**. Scale bar, 50 μ m. CT, cycle threshold; ND, not detected.

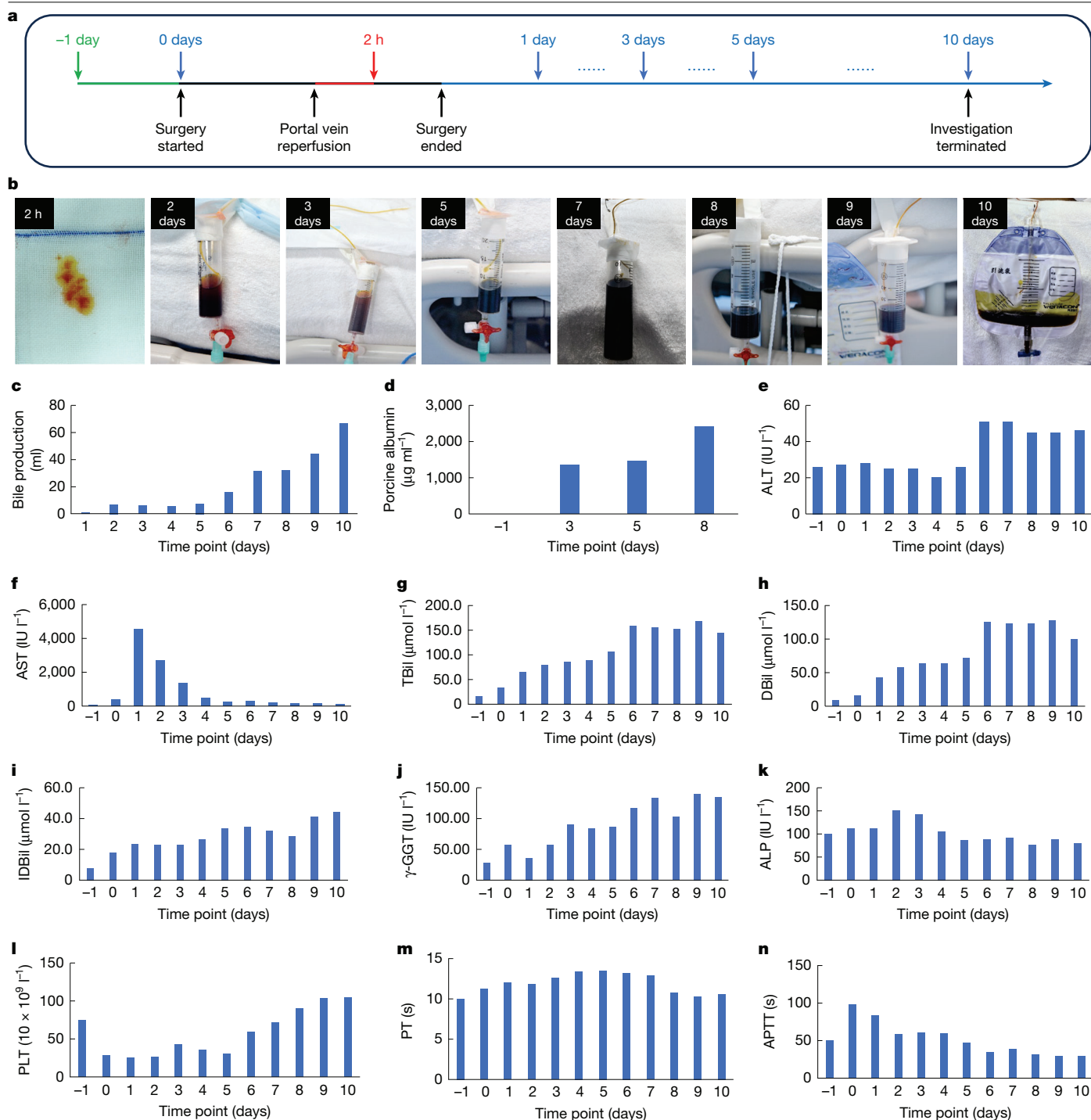


Fig. 2 | Xenograft function. **a**, Schematic depiction of the study, showing various time points of the investigation. **b**, Photographs of the bile secreted from the xenograft at different time points throughout the study. **c, d**, Amounts of bile (c) and porcine albumin (d) produced by the xenograft at different time points throughout the study. **e–k**, Amounts of ALT (e), AST (f), total bilirubin (g), direct bilirubin (h), indirect bilirubin (i), γ -GGT (j) and alkaline phosphatase (k) in the recipient’s serum at different time points throughout the study. **l–n**, Amounts of PLT (l), PT (m) and APTT (n) of the recipient at different time points throughout the study. **c–n** contain one biological and technical repetition. DBil, direct bilirubin; IDBil, indirect bilirubin; IU, international unit; TBil, total bilirubin.

concentrations of tacrolimus and mycophenolate mofetil were monitored closely throughout the study (Extended Data Fig. 7d). The xenograft was subjected to biopsy at different time points of the study. IHC staining of complements showed that little C3d, C4d and C5b-9 deposited in the xenograft throughout the investigation (Fig. 4a). By contrast, IHC staining of immunoglobulins showed that moderate amounts of IgM and IgG were detected in the xenograft on postoperative day 10 (Fig. 4b), even though no significant changes in serum

IgM or IgG were observed peri-operatively (Extended Data Fig. 7b). A panel of peripheral blood-derived immunocytes and cytokines was also assessed. Because of the administration of anti-thymocyte globulin, T cells, especially CD4^+ T cells, were inhibited at the beginning of the postoperative period, while B cells were augmented (Extended Data Fig. 7a). Beginning on day 3, rituximab was applied, which promptly reduced the B cell population. CRP and procalcitonin, which mediate inflammatory reactivity, increased initially

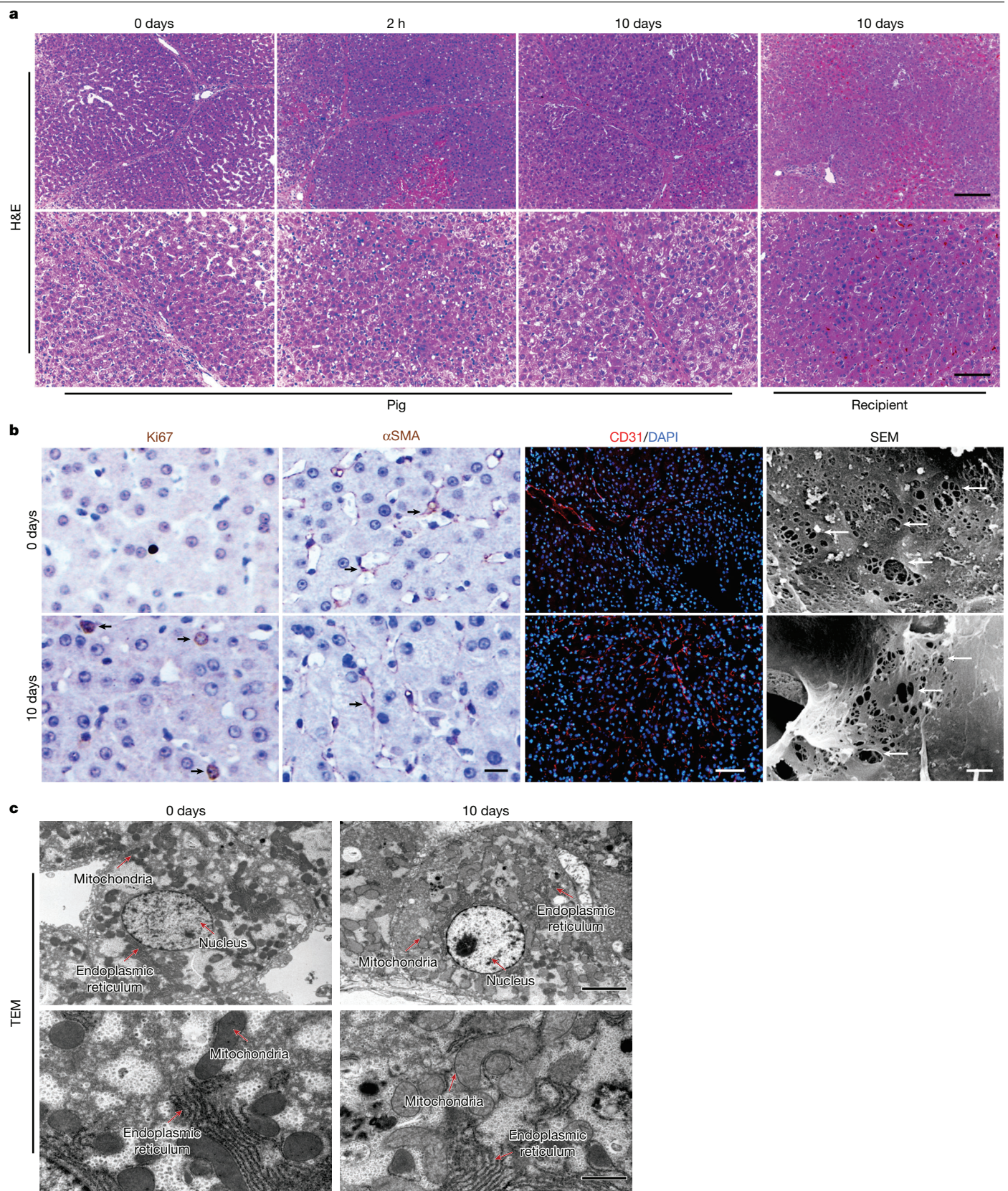


Fig. 3 | Histology of the xenograft and the original human liver.

a, Representative images of haematoxylin and eosin (H&E) staining of liver tissues obtained from the xenograft and the recipient at different time points.

b, Representative images of IHC staining of Ki67 and alpha smooth muscle actin (α SMA), immunofluorescence staining of CD31 and 4',6-diamidino-2-phenylindole (DAPI) and SEM observation of the hepatic sinusoid of the

xenograft at different time points. Positive signals are shown with black or white arrows. **c**, Representative TEM images of the porcine hepatocytes at different time points. **a–c** contain one biological and technical repetition. The experiment was carried out once in **a**, whereas two independent experiments were carried out in **b** and **c**. Scale bars, 1 μ m (**b** (right)), 4 μ m (**c** (top)), 25 μ m (**b** (left)), 100 μ m (**a** (bottom)), 200 μ m (**a**, top).

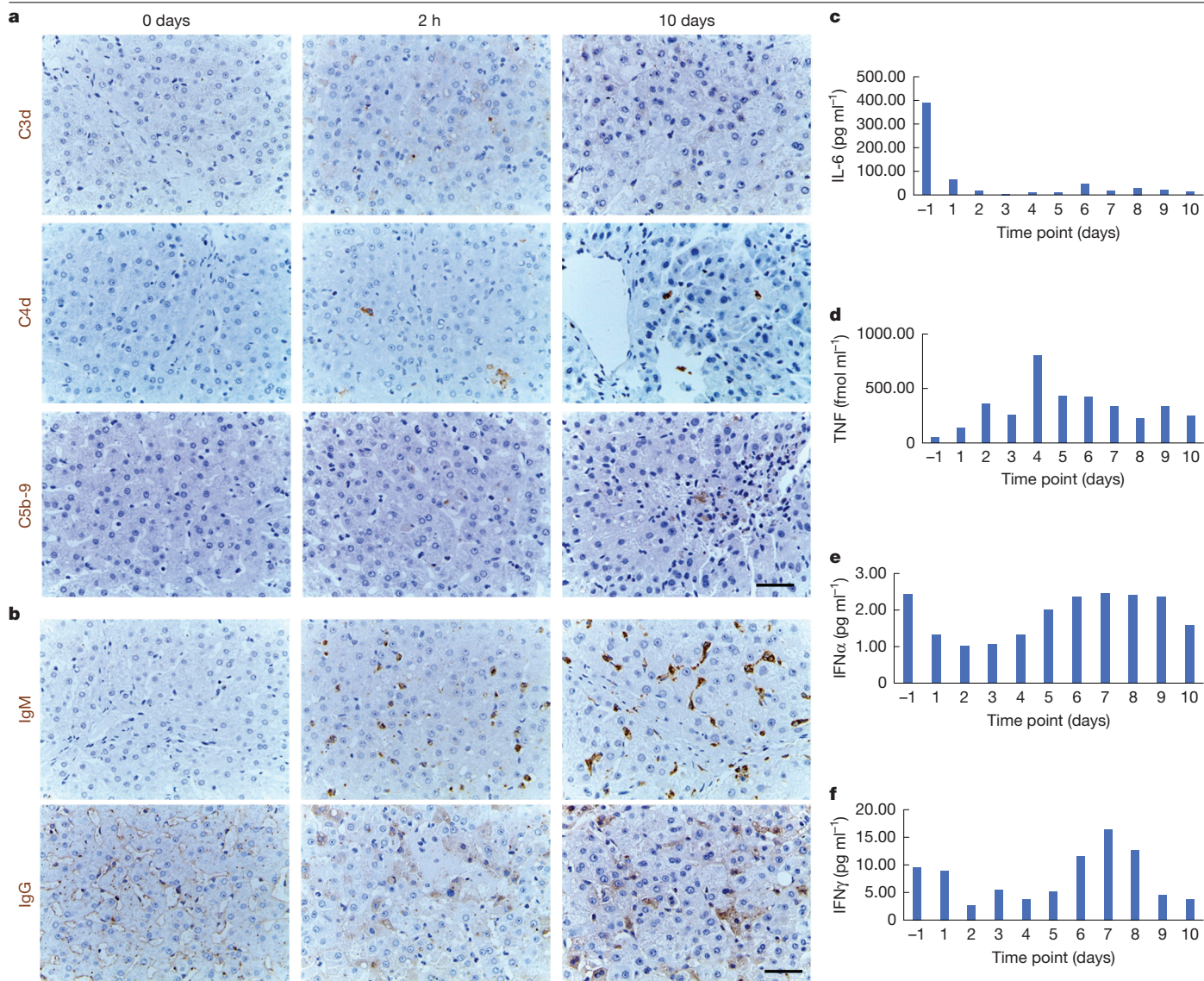


Fig. 4 | Immune and inflammatory monitoring of the recipient. **a**, Representative images of IHC staining of C3d, C4d and C5b-9 on the liver sections obtained from the xenograft at different time points of the study. **b**, Representative images of IHC staining of IgM and IgG on the liver sections obtained from the xenograft at different time points of the study. **c–f**, Amounts

of interleukin-6 (IL-6) (**c**), TNF (**d**), IFNα (**e**) and IFNγ (**f**) in the recipient's serum at different time points throughout the study. **a** and **b** contain one biological and technical repetition. For **a**, two independent experiments were carried out, whereas for **b**, the experiment was carried out once. Scale bars, 50 μm.

and then declined (Extended Data Fig. 7c). Interleukin-6 expression was maintained at a very low level postoperatively (Fig. 4c). Other cytokines, including TNF, interferon-α (IFNα) and IFNγ seemed to be suppressed at the early stage after surgery (Fig. 4d–f). These data together indicate that the inflammatory response was well controlled after transplantation.

Discussion

Xenotransplantation has entered the era of clinical research. Research teams at the University of Maryland School of Medicine have performed pig-to-human heart transplantation and scientists at both Massachusetts General Hospital and New York University recently carried out pig-to-human kidney transplantation^{3–7}. Scientists from the University of Pennsylvania used a porcine liver to treat a brain-dead person with liver failure¹². The current study was performed to preliminarily evaluate the feasibility of pig-to-human liver xenotransplantation. The use of genetic modification and a designated

pathogen-free environment may have prevented hyperacute rejection and potential PERV, PCMV or other porcine virus infections in the recipient.

As described, a heterotopic auxiliary liver transplantation was performed. To ensure the best match, the calibre and flow velocity of main blood vessels in the donor and recipient were assessed before surgery. This guaranteed sufficient blood perfusion in the xenograft and hemodynamic stability in the recipient, avoiding graft dysfunction caused by haemodynamic disorders, as reported in ref. 6. Auxiliary liver transplantation is an ideal bridge therapy for individuals with liver failure, because it is not difficult to remove pig liver and reconstruct the IVC when the function of the original liver is restored or when a suitable donor liver is available. We removed the xenograft and reconstructed the IVC at the end of the study to simulate the abovementioned situation. Moreover, our heterotopic auxiliary liver transplantation protocol improved the efficiency of interventional thrombolysis directly from the deep vein of the lower limb. The first case of pig-to-human heart xenotransplantation found microthrombi

in the terminal stage biopsies⁷. Similarly, the current study found that D-dimer levels were transiently elevated shortly after surgery (Extended Data Fig. 5a). Timely thrombolysis was then used to keep the xenograft functional.

Indeed, the flow in the infrarenal IVC is not physiological. To achieve physiological haemodynamics, we must perform auxiliary partial orthotopic liver transplantation. However, this will remove part of the original liver and may cause potential complications such as liver malfunction, bile leakage or bleeding in patients. Because our goal is to assist patients with acute liver failure through the critical period, there is no need to perform a transplantation that fully conforms to physiology. As long as the xenograft can provide metabolic and coagulation functions for a certain time, this transplantation is sufficient. In this study, we used the blood flow of the IVC to supply the xenograft, which then successfully returned to the heart. Throughout the whole study, no oedema was observed in the lower limbs, indicating that the lower limb circulation was guaranteed. More importantly, the xenograft remained functional and the haemodynamics remained stable until study completion. Therefore, non-physiological flow in this study did not cause severe disturbance.

Hyperacute rejection is one of the most critical issues with xenotransplantation in preclinical models¹⁸. Fortunately, no evidence of hyperacute rejection was found in the current study. In addition to editing the glycoprotein α -galactosyltransferase 1 gene, a series of immunosuppressive agents were used, of which tacrolimus (FK506) played a vital role. During the early stage of this xenotransplantation, we used tacrolimus at a concentration of 5 mg l⁻¹ (the upper limit of normal), according to our previous protocol. However, a high blood concentration of tacrolimus was noted at postoperative day 2, which might result from the heterogeneity of drug metabolism. We adjusted the dose in time. At the late stage of this experiment, the level of total bilirubin was elevated, which may be related to the toxicity of tacrolimus.

Whether to use Rituxan (rituximab) during induction immunosuppression was one of the focuses of our pre-operative discussion. Because of the huge advantages of gene editing, humoral immunity no longer has a major impact on graft survival. Therefore, Rituxan was not included in the immunosuppression strategy of works related to liver xenotransplantation^{19,20}. Similarly, we did not use Rituxan in our previous trails of pig-to-monkey xenotransplantation, because B cells were not activated in these studies¹³. Therefore, in this study, Rituxan was not used initially. When B cells started to be augmented, we had to adopt Rituxan, along with plasma exchange and intravenous immunoglobulin therapy, which theoretically can remove the formed antibodies and plasmacytes. This trial indicates that the activation of B cells might occur in pig-to-human liver xenotransplantation. Further investigation is needed before we can incorporate Rituxan into our induction immunosuppressive strategy.

The discrepancy in ALT and AST amounts was unexpected and something that has not been observed in previous animal studies. More interestingly, a spike in AST during the early stage was detected in a pig-to-human heart xenotransplantation performed in a previous study⁶. It is plausible that AST was released by myocardial cells. This is supported by the early increase in creatine kinase and creatinine kinase-myocardial band amounts observed at the same time point (Extended Data Fig. 7e). Consequently, myocardial damage should be assessed at the early stage of liver transplantation and pharmacological myocardial protection implemented if necessary. Notably, some cholestasis was observed in the recipient's original liver tissue on day 10, which may explain the elevated bilirubin observed later. However, this was absent in the xenograft. Thus, it is probable that current therapeutic drugs are slightly less toxic to pig liver than to human liver.

Abnormality in coagulation is a main cause of xenograft dysfunction²¹, and occurred in the first pig-to-human cardiac xenotransplantation⁷

and in our previous cases of pig-to-monkey liver xenotransplantation. However, no serious bleeding or clotting disorder occurred in the current case. PT remained relatively stable after surgery, APTT increased transiently at the early stage and later declined, and PLT decreased transiently in the early stage and later increased. Bleeding disorders and coagulopathies were considerably milder in this brain-dead recipient than in previous monkey recipients, indicating that humanized genetic modifications may function better in humans. Because of the advantages of heterotopic auxiliary liver transplantation, we were able to intervene after the early elevation of D-dimer and prevent potential PV thrombosis.

Future studies will need to choose between a bridge graft or permanent placement of xenotransplantation. Although the xenograft could secrete bile and produce porcine albumin in this study, it is unlikely that the production of bile and porcine albumin was enough to support the human body for a long period. Consequently, as indicated in ref. 17, current liver xenotransplantation modalities may be more suitable as an adjuvant bridge therapy for individuals with liver failure who are waiting for a human liver. Nevertheless, it will be important to design effective orthotopic pig-to-human liver xenotransplantation methods for future patients.

We admit the limitations of this study. First, at the request of the recipient's family members, the study was terminated on day 10, which made the follow-up period insufficient to analyse alterations in xenograft function over a long period. Second, at present, we could measure only the basic functions of the liver, such as the synthesis of albumin and the secretion of bile. However, this unique pig-to-human liver xenotransplantation can still provide critical information that cannot be provided by animal experiments alone.

Online content

Any methods, additional references, Nature Portfolio reporting summaries, source data, extended data, supplementary information, acknowledgements, peer review information; details of author contributions and competing interests; and statements of data and code availability are available at <https://doi.org/10.1038/s41586-025-08799-1>.

1. Pan, D. et al. Progress in multiple genetically modified minipigs for xenotransplantation in China. *Xenotransplantation* **26**, e12492 (2019).
2. Cooper, D. K., Ekser, B., Ramsoondar, J., Phelps, C. & Ayares, D. The role of genetically engineered pigs in xenotransplantation research. *J. Pathol.* **238**, 288–299 (2016).
3. Griffith, B. P. et al. Genetically modified porcine-to-human cardiac xenotransplantation. *N. Engl. J. Med.* **387**, 35–44 (2022).
4. Montgomery, R. A. et al. Results of two cases of pig-to-human kidney xenotransplantation. *N. Engl. J. Med.* **386**, 1889–1898 (2022).
5. Loupy, A. et al. Immune response after pig-to-human kidney xenotransplantation: a multimodal phenotyping study. *Lancet* **402**, 1158–1169 (2023).
6. Moazami, N. et al. Pig-to-human heart xenotransplantation in two recently deceased human recipients. *Nat. Med.* **29**, 1989–1997 (2023).
7. Mohiuddin, M. M. et al. Graft dysfunction in compassionate use of genetically engineered pig-to-human cardiac xenotransplantation: a case report. *Lancet* **402**, 397–410 (2023).
8. Dai, Y. et al. Targeted disruption of the alpha1,3-galactosyltransferase gene in cloned pigs. *Nat. Biotechnol.* **20**, 251–255 (2002).
9. Petersen, B. et al. Efficient production of biallelic GGTA1 knockout pigs by cytoplasmic microinjection of CRISPR/Cas9 into zygotes. *Xenotransplantation* **23**, 338–346 (2016).
10. Petersen, B. et al. Transgenic expression of human heme oxygenase-1 in pigs confers resistance against xenograft rejection during ex vivo perfusion of porcine kidneys. *Xenotransplantation* **18**, 355–368 (2011).
11. Petersen, B. et al. Pigs transgenic for human thrombomodulin have elevated production of activated protein C. *Xenotransplantation* **16**, 486–495 (2009).
12. Regalado, A. A brain-dead man was attached to a gene-edited pig liver for three days. *MIT Technology Review* www.technologyreview.com/2024/01/18/1086791/brain-dead-man-gene-edited-pig-liver/ (2024).
13. Zhang, Z. et al. Cytokine profiles in Tibetan macaques following α -1,3-galactosyltransferase-knockout pig liver xenotransplantation. *Xenotransplantation* **24**, e12321 (2017).
14. Zhang, X. et al. The resurgent landscape of xenotransplantation of pig organs in nonhuman primates. *Sci. China Life Sci.* **64**, 697–708 (2021).
15. Zhang, X. et al. A review of pig liver xenotransplantation: current problems and recent progress. *Xenotransplantation* **26**, e12497 (2019).
16. Ma, L. Xijing Hospital transplants pig's liver to monkey. *China Daily* www.chinadaily.com.cn/china/2013-06/06/content_16580042.htm (2013).

Article

17. Mallapaty, S. First pig liver transplanted into a person lasts for 10 days. *Nature* **627**, 710–711 (2024).
18. Cooper, D. K. C. et al. Xenotransplantation—the current status and prospects. *Br. Med. Bull.* **125**, 5–14 (2018).
19. Shah, J. A. et al. Prolonged survival following pig-to-primate liver xenotransplantation utilizing exogenous coagulation factors and costimulation blockade. *Am. J. Transplant.* **17**, 2178–2185 (2017).
20. Shah, J. A. et al. A bridge to somewhere. *Ann. Surg.* **263**, 1069–1071 (2016).
21. Cowan, P. J., Robson, S. C. & d'Apice, A. J. Controlling coagulation dysregulation in xenotransplantation. *Curr. Opin. Organ Transplant.* **16**, 214–221 (2011).

Publisher's note Springer Nature remains neutral with regard to jurisdictional claims in published maps and institutional affiliations.



Open Access This article is licensed under a Creative Commons Attribution-NonCommercial-NoDerivatives 4.0 International License, which permits any non-commercial use, sharing, distribution and reproduction in any medium or format, as long as you give appropriate credit to the original author(s) and the source, provide a link to the Creative Commons licence, and indicate if you modified the licensed material. You do not have permission under this licence to share adapted material derived from this article or parts of it. The images or other third party material in this article are included in the article's Creative Commons licence, unless indicated otherwise in a credit line to the material. If material is not included in the article's Creative Commons licence and your intended use is not permitted by statutory regulation or exceeds the permitted use, you will need to obtain permission directly from the copyright holder. To view a copy of this licence, visit <http://creativecommons.org/licenses/by-nc-nd/4.0/>.

© The Author(s) 2025

Methods

Recipient selection and ethical review

The recipient was an adult, who was diagnosed with brain death on 7 March 2024. The recipient maintained stable circulation and had no underlying diseases. Brain death was determined by six critical care medicine and neurosurgery experts according to World Brain Death Project-Determination of Brain Death/Death by Neurologic Criteria and the Regulations and Procedures of the National Health Commission of the People's Republic of China/Brain Injury Evaluation Quality Control Centre (PRC/NHC/BQCC), following three independent assessments. The six experts are entirely independent of the research group and have no personnel overlap or connection with each other. The study was approved by the Academic Committee (28 December 2023), Medical Ethics Committee (registration number: KY20232438-C-1, 4 January 2024), Clinical Application and Ethics Committee of Human Organ Transplantation (registration number: 20231227-1, 29 December 2023) and the Ethics Committee of Experimental Animal Welfare (registration number: IACUC2023001, 4 January 2024) of Xijing Hospital attached to the Fourth Military Medical University. After receiving a detailed overview of the study procedures, the recipient's four immediate family members signed an informed consent on 8 March 2024. In addition, none of the doctors, nurses, researchers and staff involved in the study raised any objections or complaints about the content of the study, and signed a joint agreement. The surgery was officially performed on 10 March 2024. At the request of the recipient's family, the study was artificially terminated 10 days after surgery (20 March 2024). The whole trial course was supervised by the relevant review agencies listed above. The identity information and privacy of patients and their families have been strictly kept confidential throughout this entire process. We submitted the initial paper on 5 June 2024. The files relating to ethical approval, clinical trial research protocol, informed consent for the recipient's family and determination of recipient brain death are included in the Supplementary Information.

Donor profile and xenograft acquisition

A 7-month-old male Bama miniature pig (*Sus scrofa domestica*) with six genetic modifications (*GGTA1-KO*/ β 4*GalALNT2-KO*/*CMAH-KO*/*hCD46/hCD55/hTHBD*) was used as the donor in this study. The pig was kindly provided by Clonorgan Biotechnology in Chengdu, China, and was isolated in the Laboratory Animal Center Facilities of Xijing Hospital. Flow cytometry, western blotting and IHC were used to determine whether gene editing in the donor pig occurred as expected. The donor pig underwent a comprehensive pre-operative laboratory and imaging examination by a multidisciplinary team to confirm it was compatible with the recipient. The porcine liver, weighing 700 g, was obtained in a sterile surgical environment. The donor pig was anaesthetized and a median incision was made in the abdomen to expose the abdominal aorta, IVC, liver, kidney, PV, hepatic artery, bile duct, and so on. The abdominal aorta was perfused with 2,000 ml of hypertonic citrate purine solution (Shanghai Blood Transfusion Technology Co., Ltd) and 1,000 ml of Celsior solution (flushing and cold storage solution for

solid organ preservation; Institut Georges Lopez S.A.S.) at 0–4 °C. IVC drainage was performed. The PV was intubated with 2,000 ml of Celsior solution at 0–4 °C. Sterile ice cubes were used to cool the liver. After adequate perfusion with Celsior solution at 0–4 °C, the liver was excised and trimmed in 1,000 ml of the same solution before implantation.

Heterotopic auxiliary liver transplant

The recipient was routinely anaesthetized and sterilized, and a cross-like abdominal incision was made (Extended Data Fig. 3c). The abdominal aorta and IVC were dissociated and the IVC was transected below the level of the right renal vein. Subsequently, the supra-hepatic IVC of the donor liver was connected to the proximal end of the recipient's IVC and the porcine PV was anastomosed with the distal end of the transected IVC. After reperfusion of the PV blood flow, the porcine liver looked ruddy with a good texture, and goldish bile began to flow shortly thereafter. The hepatic artery of the donor liver was then opened after its end-to-side anastomosis with the recipient's abdominal aorta. The bile was drained out of the body and two abdominal drains were placed (Extended Data Fig. 3c). At the end of the study (day 10), the xenograft was surgically removed and the IVC was reconstructed using an artificial vessel. A video of the detailed surgical procedures is included in the Supplementary Information.

Reporting summary

Further information on research design is available in the Nature Portfolio Reporting Summary linked to this article.

Data availability

FACS gating strategies and full scans of all the gels as well as blots are provided in Supplementary Figs. 1–3. The data that support the findings of this study are available from the corresponding author upon reasonable request. Source data are provided with this paper.

Acknowledgements This work was supported by grants from National Natural Science Foundation of China (grant nos. 82325007, 92468202, 82371793, 82070671, 82170667) and the National Key Research and Development Program of China (grant no. 2021YFA1100502).

Author contributions K.-S.T. and Z.-X.Y. conducted the surgery with the participation of S.-Q.Y., Y.-L.Y., W.-J.S., D.-S.W., Z.-C.L., H.-M.L., Y.C. and R.D. X.Z. prepared the donor pig and collected the experimental data. H.-T.Z. monitored the patient throughout the investigation. S.-R.S., M.Y., J.-P.L., W.-X.D., Z.W., J.-W.W., J.-Y.L., M.-W.Z., X.-J.Z., W.Y., W.-J.Q., D.-M.B., L.L. and M.L. assisted with the surgery and recipient management. Z.-B.L., H.X. and D.W. prepared the draft of the manuscript. H.Z. and J.-L.D. undertook the histological observation. D.-K.P. established the gene-edited donor pig. L.W. planned and wrote the article. H.-L.D., L.W. and K.-F.D. designed and supervised the whole study.

Competing interests The authors declare no competing interests.

Additional information

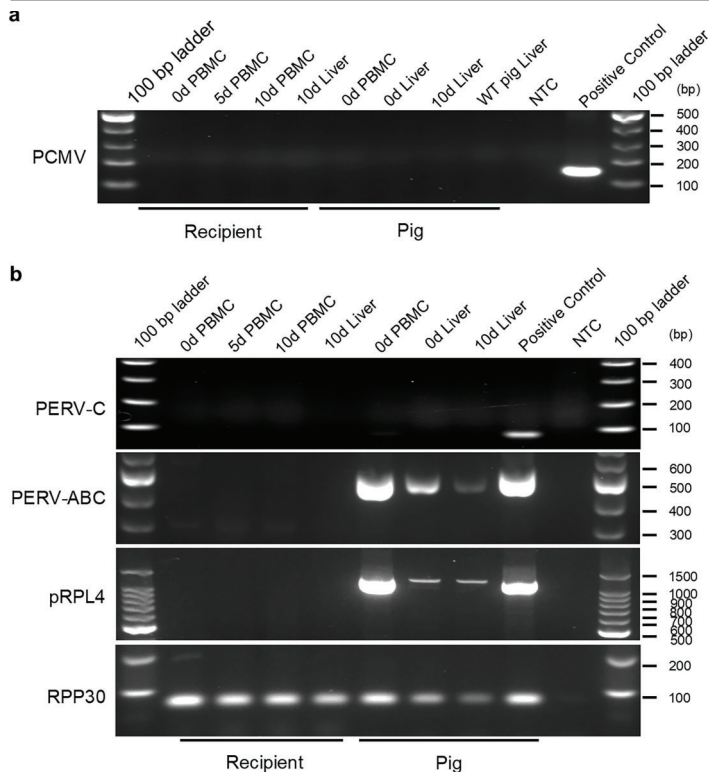
Supplementary information The online version contains supplementary material available at <https://doi.org/10.1038/s41586-025-08799-1>.

Correspondence and requests for materials should be addressed to Hai-Long Dong, Lin Wang or Ke-Feng Dou.

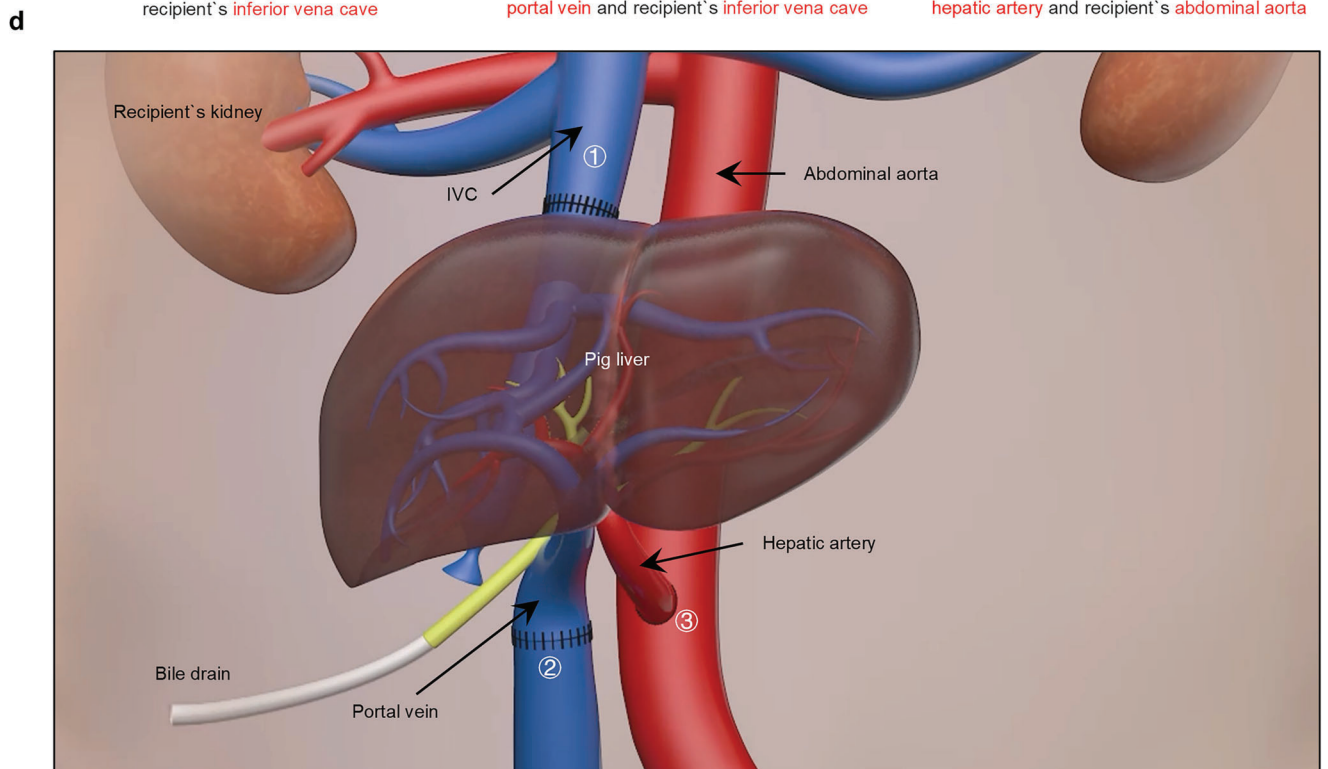
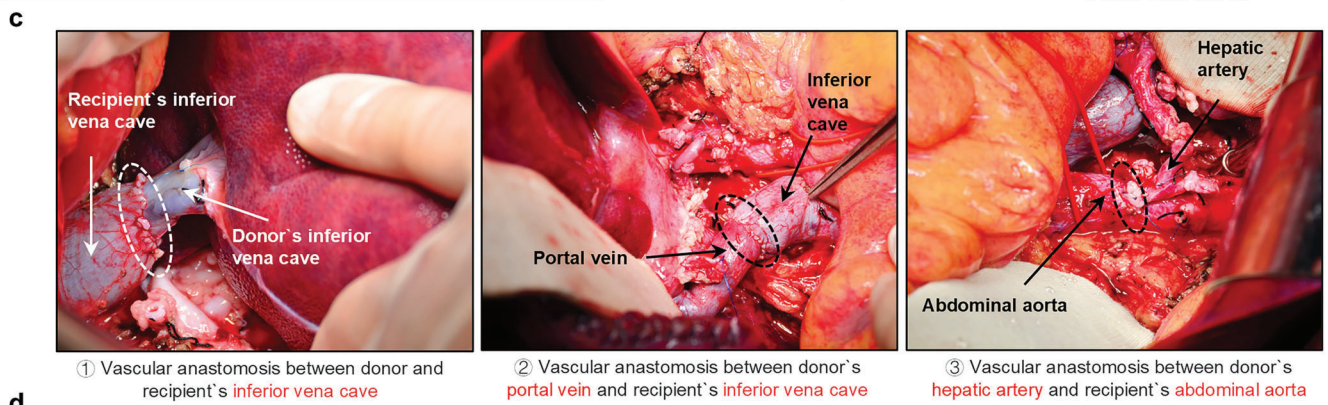
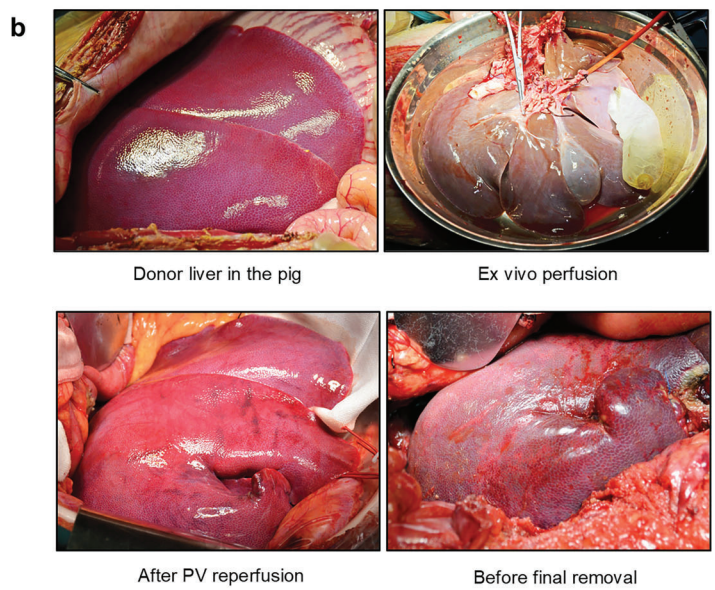
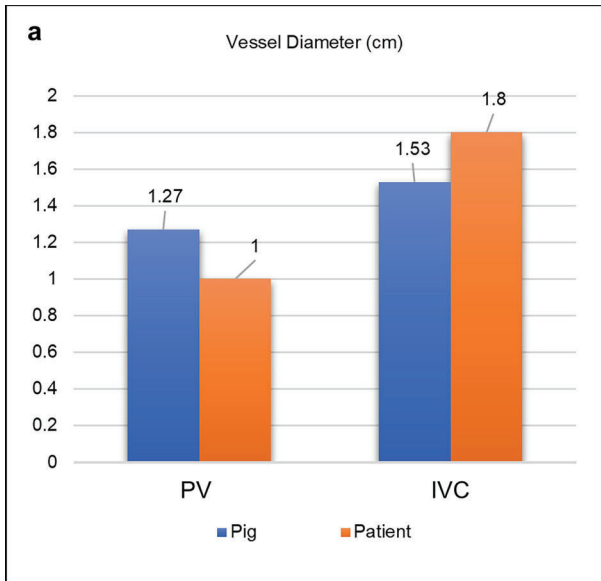
Peer review information Nature thanks Arthur Caplan, Muhammad Mohiuddin and the other, anonymous, reviewer(s) for their contribution to the peer review of this work.

Reprints and permissions information is available at <http://www.nature.com/reprints>.

Article



Extended Data Fig. 1 | Pathogenic surveillance of the donor pig. a, The PCR combined with gel electrophoresis detecting the presence of PCMV in the PBMCs of the recipient and the xenograft. **b,** The PCR combined with gel electrophoresis detecting the presence of PERV as well as microchimerism in the PBMCs of the recipient and the xenograft. PERV-ABC, the sequence shared by PERV-A, PERV-B and PERV-C. PERV-C, the sequence specifically belongs to PERV-C. RPP30 was used as the control gene. NTC, no template control. For gel source data, see Supplementary Fig. 1. Extended Data Fig. 1a,b contains 1 biological and technical repetition, and 3 independent experiments were carried out.

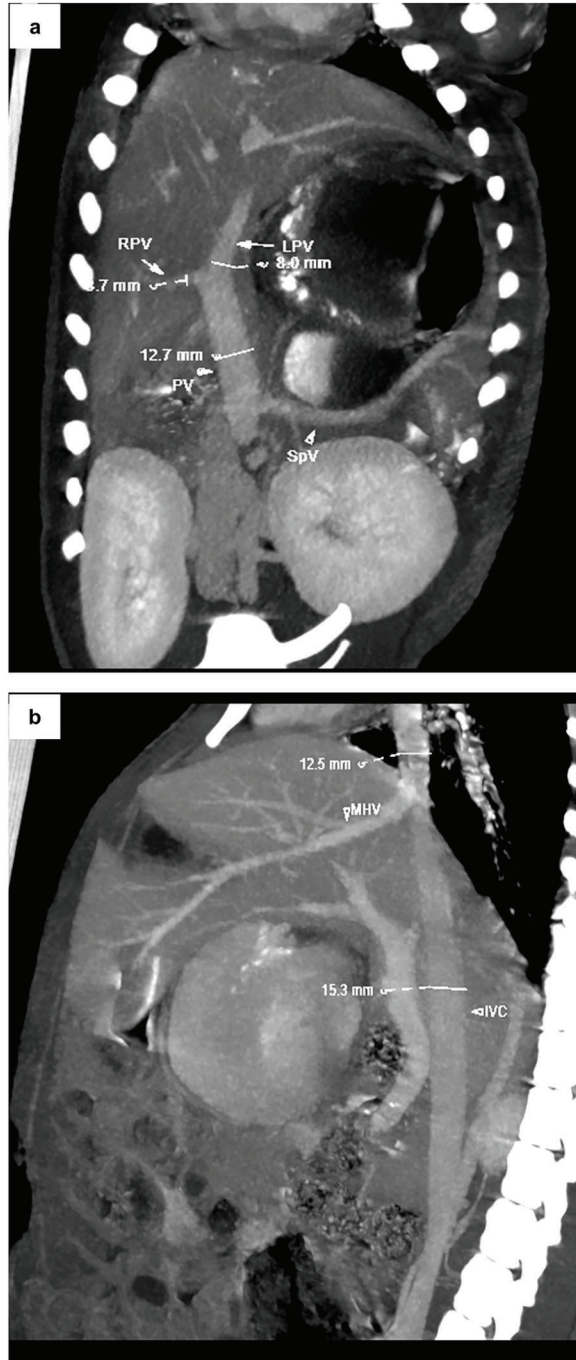


Extended Data Fig. 2 | The heterotopic auxiliary liver xenotransplantation procedure. **a**, The diameters of the portal vein (PV) and the inferior vena cava (IVC) of the recipient and the donor pig detected by vessel segmentation and ultrasound. **b**, Photos of the donor liver at different time points throughout the

study. **c**, Photos of the vascular anastomosis between the recipient and the donor liver during surgery. **d**, A schematic depiction of the surgery. ①, ② and ③ represent the vascular anastomosis captioned in **c**.

Article

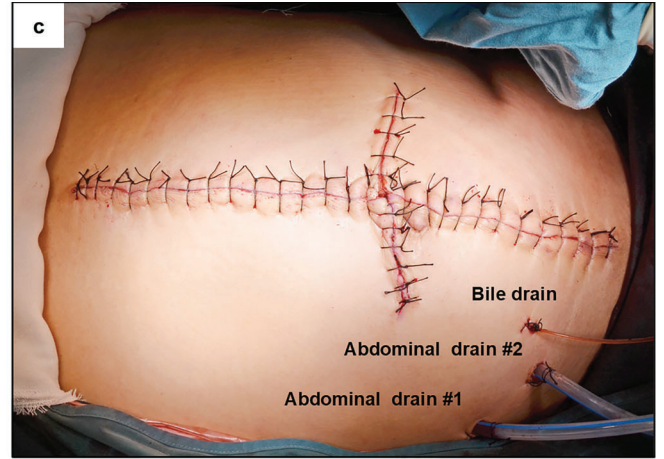
Vessel segmentation



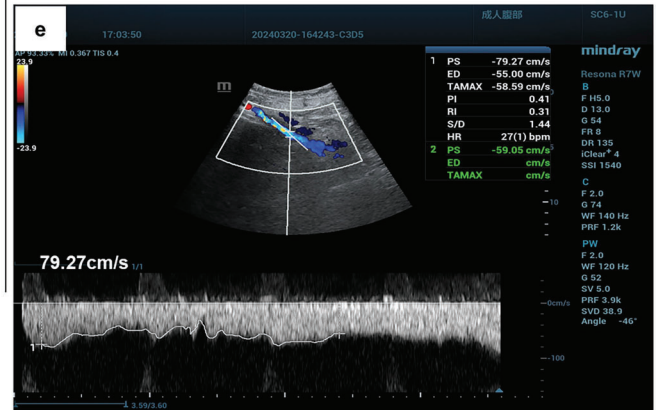
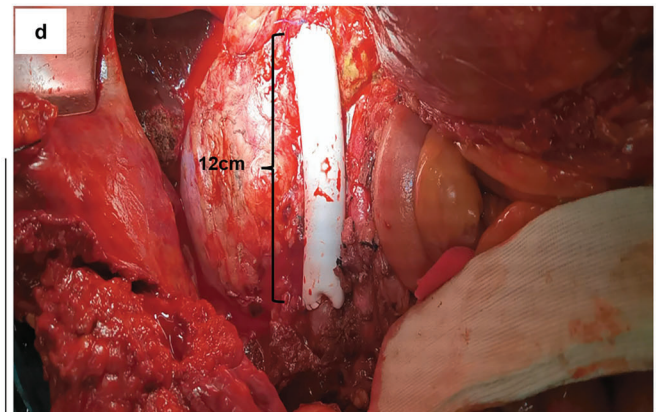
Pig

Extended Data Fig. 3 | Other surgery details. **a, b**, Images of vessel segmentation in the donor pig. **c**, A photo of the recipient's abdomen, showing the surgical incision, abdominal drains, and bile drain. **d**, A photo of the reconstruction of

Surgical incision

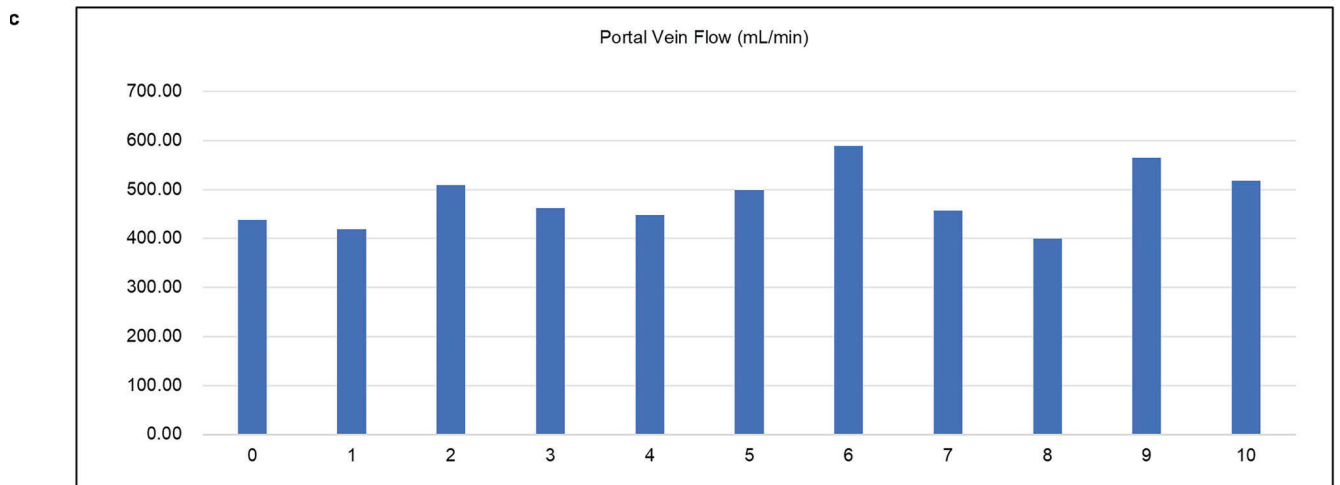
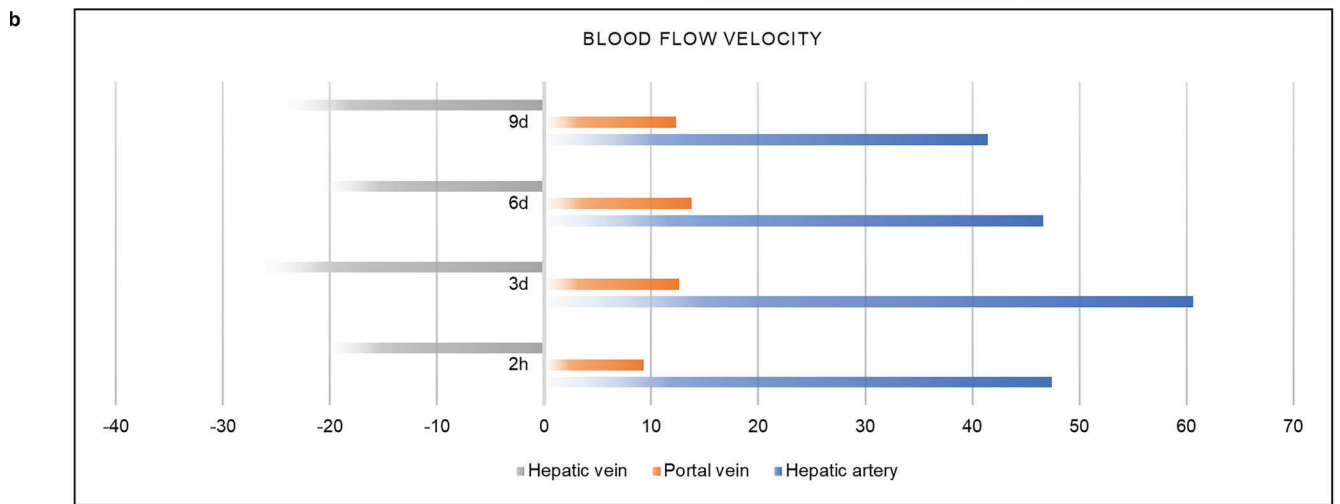
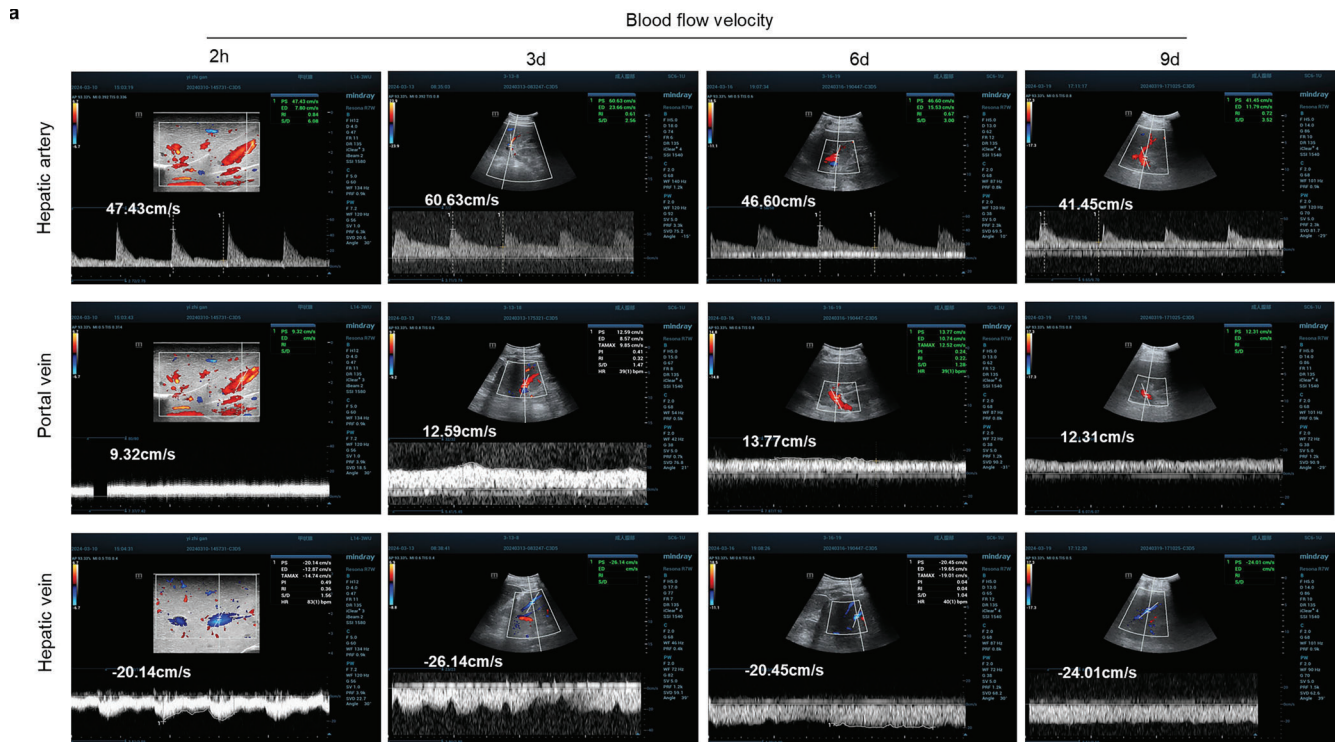


Reconstruction of IVC



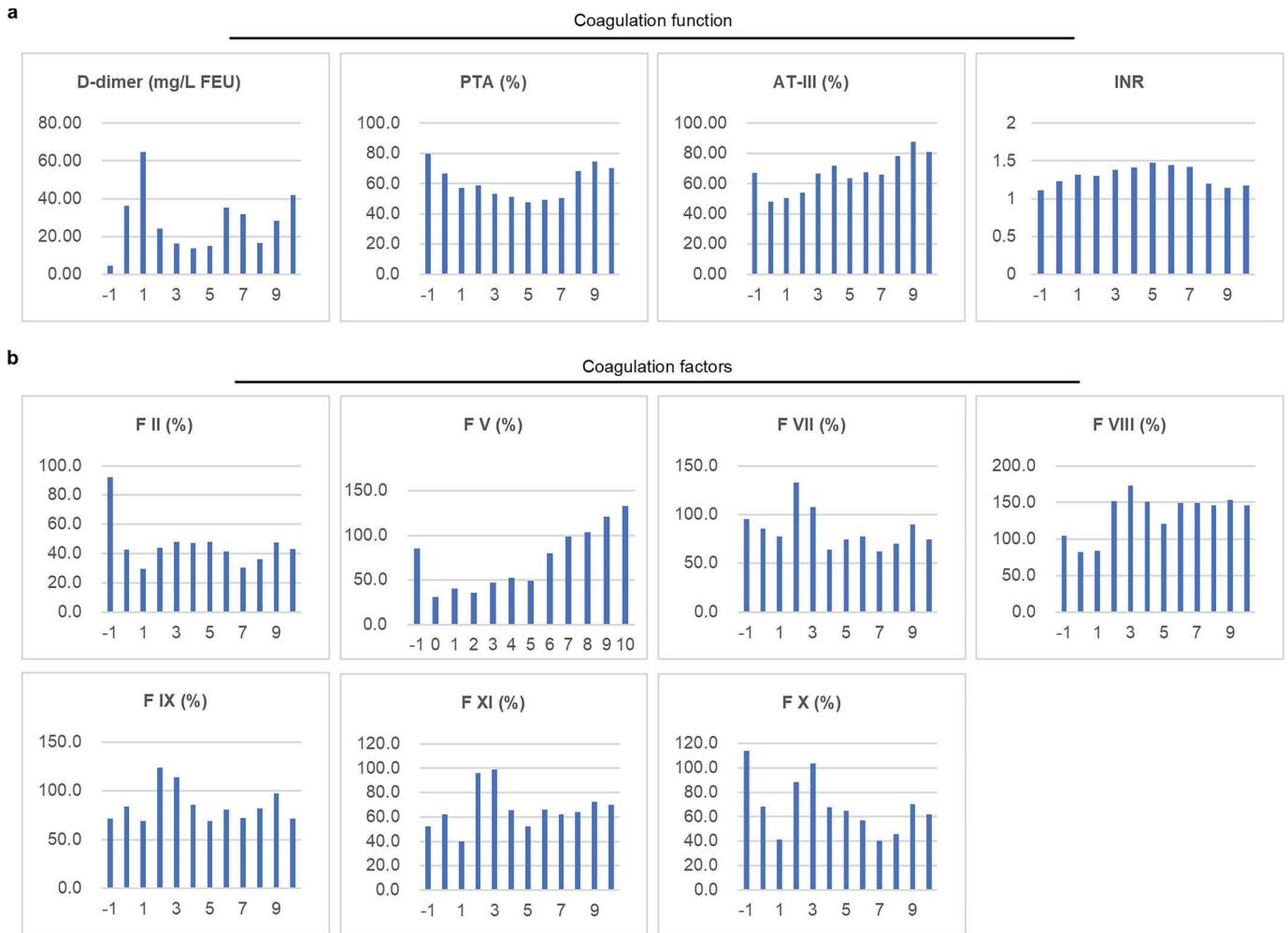
Patient

the recipient's IVC by artificial vessel once the porcine liver was removed. **e**, The ultrasound-detected blood flow velocity of IVC after artificial vessel reconstruction.



Extended Data Fig. 4 | Hemodynamic monitoring of the xenograft. a, The ultrasound-detected blood flow velocity of the hepatic artery, the portal vein, and the hepatic vein of the xenograft at different time points of the study. The

exact speed of blood flow is labelled correspondingly. **b,** The quantitative result of **a.** **c,** The ultrasound-detected portal vein flow (PVF) of the xenograft at different time points of the study.

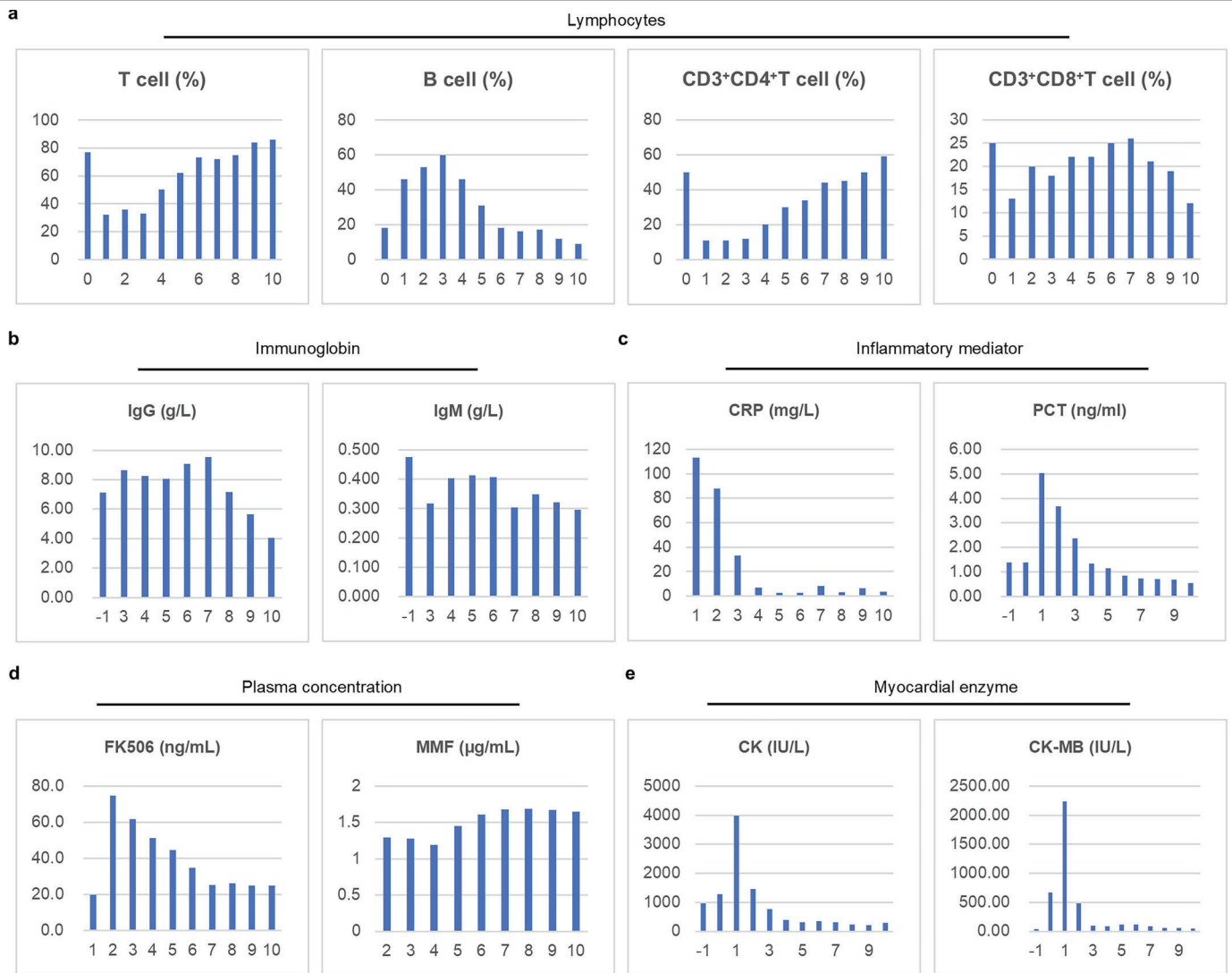


Extended Data Fig. 5 | Bleeding and coagulation monitoring of the recipient. **a**, The indicators of coagulation function of the recipient at different time points of the study. **b**, The serum levels of coagulation factors of the recipient at different time points of the study. Extended Data Fig. 5a,b contains 1 biological and technical repetition.

Immunosuppression strategy

	-1d	0d	1d	2d	3d	4d	5d	6d	7d	8d	9d	10d
ATG	75mg	75mg Pre-Tx										
Ravulizumab		90ml Pre-Tx										
Etanercept		25mg/0.47ml Pre-Tx			25mg /0.47ml				25mg /0.47ml			
Methyl- prednisolone	40mg	650mg before perfusion 650mg Post-Tx	1500mg	1500mg	1500mg	750mg	750mg	750mg	375mg	375mg	375mg	190mg
MMF		1g Post-Tx	1g 2/d	1g 2/d	1g 2/d	1g 2/d	1g 2/d	1g 2/d	1g 2/d	1g 2/d	1g 2/d	1g
Tacrolimus (FK506)		3.9mg Pre-Tx	5mg 2/d	5mg 2.5mg	1.67mg 1.25mg	1.25mg 1.25mg	1.25mg 1.25mg	1.25mg 0.8mg	0.8mg 0.8mg	0.8mg 0.8mg	0.8mg 0.6mg	0.6mg
Rituximab					100mg	200mg	200mg					

Extended Data Fig. 6 | Immune strategy of the recipient. The immunosuppression strategy adopted in this study.



Extended Data Fig. 7 | Immune monitoring of the recipient. **a**, The levels of total T, B, CD3⁺CD4⁺ T and CD3⁺CD8⁺ T cells in the recipient's blood at different time points of the study. **b**, The levels of IgM and IgG in the serum of the recipient at different time points of the study. **c**, The levels of C-reactive protein (CRP) and procalcitonin (PCT) in the serum of the recipient at different time points of

the study. **d**, The plasma concentrations of FK506 and mycophenolate mofetil (MMF) of the recipient at different time points of the study. **e**, The serum levels of myocardial enzymes of the recipient at different time points of the study. Extended Data Fig. 7a–e contains 1 biological and technical repetition.

Reporting Summary

Nature Portfolio wishes to improve the reproducibility of the work that we publish. This form provides structure for consistency and transparency in reporting. For further information on Nature Portfolio policies, see our [Editorial Policies](#) and the [Editorial Policy Checklist](#).

Statistics

For all statistical analyses, confirm that the following items are present in the figure legend, table legend, main text, or Methods section.

n/a Confirmed

- The exact sample size (n) for each experimental group/condition, given as a discrete number and unit of measurement
- A statement on whether measurements were taken from distinct samples or whether the same sample was measured repeatedly
- The statistical test(s) used AND whether they are one- or two-sided
Only common tests should be described solely by name; describe more complex techniques in the Methods section.
- A description of all covariates tested
- A description of any assumptions or corrections, such as tests of normality and adjustment for multiple comparisons
- A full description of the statistical parameters including central tendency (e.g. means) or other basic estimates (e.g. regression coefficient) AND variation (e.g. standard deviation) or associated estimates of uncertainty (e.g. confidence intervals)
- For null hypothesis testing, the test statistic (e.g. F , t , r) with confidence intervals, effect sizes, degrees of freedom and P value noted
Give P values as exact values whenever suitable.
- For Bayesian analysis, information on the choice of priors and Markov chain Monte Carlo settings
- For hierarchical and complex designs, identification of the appropriate level for tests and full reporting of outcomes
- Estimates of effect sizes (e.g. Cohen's d , Pearson's r), indicating how they were calculated

Our web collection on [statistics for biologists](#) contains articles on many of the points above.

Software and code

Policy information about [availability of computer code](#)

Data collection Images of gels and blots were obtained by Image Lab Software. Images of IHC and HE staining were obtained by LAC V4.8. software. FACS data were obtained by Cell Sorter Software Version 3.2.0. Images of SEM were obtained by XT microscopeServer21.0.0. Images of TEM were obtained by RADIUS.

Data analysis FACS data were analyzed by Flowjo V10.8.1.

For manuscripts utilizing custom algorithms or software that are central to the research but not yet described in published literature, software must be made available to editors and reviewers. We strongly encourage code deposition in a community repository (e.g. GitHub). See the Nature Portfolio [guidelines for submitting code & software](#) for further information.

Data

Policy information about [availability of data](#)

All manuscripts must include a [data availability statement](#). This statement should provide the following information, where applicable:

- Accession codes, unique identifiers, or web links for publicly available datasets
- A description of any restrictions on data availability
- For clinical datasets or third party data, please ensure that the statement adheres to our [policy](#)

FACS gating strategies and full scans of all the gels as well as blots are provided in Supplementary Figures. All source data underlying the graphs are provided in the Source Data. The data that support the findings of this study are available from the corresponding author upon reasonable request.

We did not generate any sequencing data or code in this article, and all source data can be found in the Supplementary Information or Supplementary Data. Hence, we did not upload them in a repository.

Research involving human participants, their data, or biological material

Policy information about studies with [human participants or human data](#). See also policy information about [sex, gender \(identity/presentation\), and sexual orientation](#) and [race, ethnicity and racism](#).

Reporting on sex and gender	Only one human participant in this study.
Reporting on race, ethnicity, or other socially relevant groupings	Race: Asian; Ethnicity: Chinese
Population characteristics	cause of death: a severe closed head injury
Recruitment	A recipient with stable vital signs and no pre-existing underlying disease experienced a severe closed head injury and was determined to be brain dead by six critical care medicine and neurosurgery experts according to World Brain Death Project-Determination of Brain Death/Death by Neurologic Criteria and the Regulations and Procedures of the National Health Commission of the People's Republic of China/ Brain Injury Evaluation Quality Control Centre (PRC/NHC/BQCC), following three independent assessments.
Ethics oversight	The study was approved by the Academic Committee, Medical Ethics Committee (Reg. No. KY20232438-C-1), Clinical Application and Ethics Committee of Human Organ Transplantation (Reg. No. 20231227-1), and the Ethics Committee of Experimental Animal Welfare (Reg. No. IACUC2023001) of Xijing Hospital attached to the Fourth Military Medical University.

Note that full information on the approval of the study protocol must also be provided in the manuscript.

Field-specific reporting

Please select the one below that is the best fit for your research. If you are not sure, read the appropriate sections before making your selection.

Life sciences Behavioural & social sciences Ecological, evolutionary & environmental sciences

For a reference copy of the document with all sections, see [nature.com/documents/nr-reporting-summary-flat.pdf](https://www.nature.com/documents/nr-reporting-summary-flat.pdf)

Life sciences study design

All studies must disclose on these points even when the disclosure is negative.

Sample size	The sample of this study is precious, that is, there is only one patient, and one tube of blood is taken at one time point for the experiment, so there is only one biological repetition and one technical repetition.
Data exclusions	No data were excluded from the analyses in this study.
Replication	We have conducted several times of independent experiments to replicate some of our results, and the number of them were provided in the figure legends.
Randomization	There are only one sample in this study, so the randomization is not applicable.
Blinding	All of the in vitro experiments were independently performed by different individuals in a blinded fashion.

Behavioural & social sciences study design

All studies must disclose on these points even when the disclosure is negative.

Study description	
Research sample	
Sampling strategy	
Data collection	
Timing	
Data exclusions	

Non-participation

Randomization

Ecological, evolutionary & environmental sciences study design

All studies must disclose on these points even when the disclosure is negative.

Study description

Research sample

Sampling strategy

Data collection

Timing and spatial scale

Data exclusions

Reproducibility

Randomization

Blinding

Did the study involve field work? Yes No

Field work, collection and transport

Field conditions

Location

Access & import/export

Disturbance

Reporting for specific materials, systems and methods

We require information from authors about some types of materials, experimental systems and methods used in many studies. Here, indicate whether each material, system or method listed is relevant to your study. If you are not sure if a list item applies to your research, read the appropriate section before selecting a response.

Materials & experimental systems

n/a	Included in the study
<input type="checkbox"/>	<input checked="" type="checkbox"/> Antibodies
<input checked="" type="checkbox"/>	<input type="checkbox"/> Eukaryotic cell lines
<input checked="" type="checkbox"/>	<input type="checkbox"/> Palaeontology and archaeology
<input type="checkbox"/>	<input checked="" type="checkbox"/> Animals and other organisms
<input checked="" type="checkbox"/>	<input type="checkbox"/> Clinical data
<input checked="" type="checkbox"/>	<input type="checkbox"/> Dual use research of concern
<input checked="" type="checkbox"/>	<input type="checkbox"/> Plants

Methods

n/a	Included in the study
<input checked="" type="checkbox"/>	<input type="checkbox"/> ChIP-seq
<input type="checkbox"/>	<input checked="" type="checkbox"/> Flow cytometry
<input checked="" type="checkbox"/>	<input type="checkbox"/> MRI-based neuroimaging

Antibodies

Antibodies used

CD55 monoclonal antibody (Santa-cruz# SC-59092PE)
 CD46 monoclonal antibody (Abnova# MAB4439)
 CD55 Polyclonal antibody (Proteintech#26580-1-AP)
 CD46 Polyclonal antibody (Proteintech #12494-1-AP)
 TBM monoclonal antibody (Proteintech #67831-1-Ig)
 GAPDH Monoclonal antibody (Proteintech#60004-1-Ig)
 Goat anti-Human IgG (H+L) Cross-Adsorbed Secondary Antibody, Alexa Fluor 488 (Invitrogen# A11013)
 Goat anti-Human IgM (Heavy chain) Cross-Adsorbed Secondary Antibody, Alexa Fluor 647 (Invitrogen# A21249)
 C3d monoclonal antibody (NOVUS# NBP3-07741)
 C4d monoclonal antibody (NOVUS# NBP2-34234)
 C5b-9 Polyclonal antibody (Abcam# ab55811)
 IgM monoclonal antibody (Abcam# ab200541)
 IgG monoclonal antibody (Abcam# ab109489)
 Ki-67 Polyclonal antibody (Proteintech#27309-1-AP)
 Smooth muscle actin specific Recombinant antibody (Proteintech # 80008-1-RR)
 CD31 monoclonal antibody (BIO-RAD # MCA1746GA)

Validation

All antibodies are commercially available and validated by the manufacturer:
 Isolectin BSI-B4 (SIGMA# L2895): <https://www.sigmaaldrich.cn/CN/zh/product/sigma/l2895> Dilution: 1:500
 Dolichos Biflorus Agglutinin (DBA) (Vector# FL-1031): <https://vectorlabs.com/products/fluorescein-dolichos-biflorus-agglutinin>.
 Dilution: 1:500
 Neu5Gc Polyclonal antibody (Biolegend#146901): <https://www.biolegend.com/en-us/products/anti-neu5gc-antibody-kit-9026>
 Dilution: 1:200
 Goat Anti-Chicken IgY H&L (DyLight® 488) (Abcam# ab96947): <https://www.abcam.cn/products/secondary-antibodies/goat-chicken-igy-hl-dylight-488-ab96947.html> Dilution: 1:200
 CD55 monoclonal antibody (Santa-cruz# SC-59092PE): https://www.scbt.com/zh/p/cd55-antibody-bric-216_5ul/106_cells
 CD46 monoclonal antibody (Abnova# MAB4439): https://www.abnova.com/zh-cn/product/detail/mab4439_10ul/106_cells
 CD55 Polyclonal antibody (Proteintech#26580-1-AP): <https://www.ptgcn.com/products/CD55-Antibody-26580-1-AP.htm>
 WB(1:5000), IHC-P(1:200)
 CD46 Polyclonal antibody (Proteintech #12494-1-AP): <https://www.ptgcn.com/products/CD46-Antibody-12494-1-AP.htm>
 WB(1:2000), IHC-P(1:500)
 TBM monoclonal antibody (Proteintech #67831-1-Ig) <https://www.ptgcn.com/products/THBD-Antibody-67831-1-Ig.htm> Dilution:
 1:500
 GAPDH Monoclonal antibody (Proteintech#60004-1-Ig) <https://www.ptgcn.com/products/GAPDH-Antibody-60004-1-Ig.htm>
 Dilution: 1:20000
 Goat anti-Human IgG (H+L) Cross-Adsorbed Secondary Antibody, Alexa Fluor 488 (Invitrogen# A11013): <https://www.thermofisher.cn/cn/zh/antibody/product/Goat-anti-Human-IgG-H-L-Cross-Adsorbed-Secondary-Antibody-Polyclonal/A-11013>
 Dilution: 1:200
 Goat anti-Human IgM (Heavy chain) Cross-Adsorbed Secondary Antibody, Alexa Fluor 647 (Invitrogen# A21249): <https://www.thermofisher.cn/cn/zh/antibody/product/Goat-anti-Human-IgM-Heavy-chain-Cross-Adsorbed-Secondary-Antibody-Polyclonal/A-21249> Dilution: 1:200
 C3d monoclonal antibody (NOVUS# NBP3-07741): https://www.novusbio.com/products/complement-c3d-antibody-c3d-2891_nbp3-07741 Dilution: 1:150
 C4d monoclonal antibody (NOVUS# NBP2-34234): https://www.novusbio.com/products/complement-c4d-antibody-c4d204_nbp2-34234 Dilution: 1:200
 C5b-9 Polyclonal antibody (Abcam# ab55811): <https://www.abcam.cn/products/primary-antibodies/c5b-9-antibody-ab55811.html>
 Dilution: 1:1000
 IgM monoclonal antibody (Abcam# ab200541): <https://www.abcam.cn/products/primary-antibodies/human-igm-antibody-im260-ab200541.html> Dilution: 1:100
 IgG monoclonal antibody (Abcam# ab109489): <https://www.abcam.cn/products/primary-antibodies/human-igg-antibody-epr4421-ab109489.html> Dilution: 1:1000
 Ki-67 Polyclonal antibody (Proteintech#27309-1-AP): <https://www.ptgcn.com/products/KI67-Antibody-27309-1-AP.htm> Dilution:
 1:500
 smooth muscle actin specific Recombinant antibody (Proteintech # 80008-1-RR): <https://www.ptgcn.com/products/a-SMA-specific-Antibody-80008-1-RR.htm> Dilution: 1:400
 CD31 monoclonal antibody (BIO-RAD # MCA1746GA): <https://www.bio-rad-antibodies.com/monoclonal/pig-porcine-cd31-antibody-lci-4-mca1746.html> Dilution: 1:50

Eukaryotic cell lines

Policy information about [cell lines and Sex and Gender in Research](#)

Cell line source(s)

Authentication

Mycoplasma contamination

Commonly misidentified lines
 (See [ICLAC](#) register)

Palaeontology and Archaeology

Specimen provenance

Specimen deposition

Dating methods

Tick this box to confirm that the raw and calibrated dates are available in the paper or in Supplementary Information.

Ethics oversight

Note that full information on the approval of the study protocol must also be provided in the manuscript.

Animals and other research organisms

Policy information about [studies involving animals](#); [ARRIVE guidelines](#) recommended for reporting animal research, and [Sex and Gender in Research](#)

Laboratory animals

Wild animals

Reporting on sex

Field-collected samples

Ethics oversight

Note that full information on the approval of the study protocol must also be provided in the manuscript.

Clinical data

Policy information about [clinical studies](#)

All manuscripts should comply with the ICMJE [guidelines for publication of clinical research](#) and a completed [CONSORT checklist](#) must be included with all submissions.

Clinical trial registration

Study protocol

Data collection

Outcomes

Dual use research of concern

Policy information about [dual use research of concern](#)

Hazards

Could the accidental, deliberate or reckless misuse of agents or technologies generated in the work, or the application of information presented in the manuscript, pose a threat to:

- | No | Yes |
|--------------------------|---|
| <input type="checkbox"/> | <input type="checkbox"/> Public health |
| <input type="checkbox"/> | <input type="checkbox"/> National security |
| <input type="checkbox"/> | <input type="checkbox"/> Crops and/or livestock |
| <input type="checkbox"/> | <input type="checkbox"/> Ecosystems |
| <input type="checkbox"/> | <input type="checkbox"/> Any other significant area |

Experiments of concern

Does the work involve any of these experiments of concern:

- | No | Yes |
|--------------------------|--|
| <input type="checkbox"/> | <input type="checkbox"/> Demonstrate how to render a vaccine ineffective |
| <input type="checkbox"/> | <input type="checkbox"/> Confer resistance to therapeutically useful antibiotics or antiviral agents |
| <input type="checkbox"/> | <input type="checkbox"/> Enhance the virulence of a pathogen or render a nonpathogen virulent |
| <input type="checkbox"/> | <input type="checkbox"/> Increase transmissibility of a pathogen |
| <input type="checkbox"/> | <input type="checkbox"/> Alter the host range of a pathogen |
| <input type="checkbox"/> | <input type="checkbox"/> Enable evasion of diagnostic/detection modalities |
| <input type="checkbox"/> | <input type="checkbox"/> Enable the weaponization of a biological agent or toxin |
| <input type="checkbox"/> | <input type="checkbox"/> Any other potentially harmful combination of experiments and agents |

Plants

Seed stocks	<input type="text"/>
Novel plant genotypes	<input type="text"/>
Authentication	<input type="text"/>

ChIP-seq

Data deposition

- Confirm that both raw and final processed data have been deposited in a public database such as [GEO](#).
- Confirm that you have deposited or provided access to graph files (e.g. BED files) for the called peaks.

Data access links <i>May remain private before publication.</i>	<input type="text"/>
Files in database submission	<input type="text"/>
Genome browser session (e.g. UCSC)	<input type="text"/>

Methodology

Replicates	<input type="text"/>
Sequencing depth	<input type="text"/>
Antibodies	<input type="text"/>
Peak calling parameters	<input type="text"/>
Data quality	<input type="text"/>
Software	<input type="text"/>

Flow Cytometry

Plots

Confirm that:

- The axis labels state the marker and fluorochrome used (e.g. CD4-FITC).
- The axis scales are clearly visible. Include numbers along axes only for bottom left plot of group (a 'group' is an analysis of identical markers).
- All plots are contour plots with outliers or pseudocolor plots.
- A numerical value for number of cells or percentage (with statistics) is provided.

Methodology

Sample preparation

PBMCs were extracted from the anticoagulant pig blood. The non-specific binding sites were blocked. Then the samples were incubated with corresponding antibodies and isotype controls, according to the manufacturer's instructions. After antibody incubating, the cells were washed twice and uploaded in a SONY MA900 flow cytometer. FlowJo 10.8.1 Software was used to analyze the data.

Instrument

SONY MA900 flow cytometer.

Software

Data were collected using Cell Sorter Software Version 3.2.0 and analysed using FlowJo 10.8.1 Software tools

Cell population abundance

In IgG and IgM binding assay, forward-scatter and side-scatter gating was used to identify pig lymphocytes on the basis of size and granularity. The binding ability of IgG and IgM was analyzed in the lymphocytes gate.

Gating strategy

FSC-A vs. SSC-A graph were used to screen the main cells population. FSC-A vs. FSC-H graph were used to select the single events. All the gating strategies used in this article are included in supplementary Figures.

- Tick this box to confirm that a figure exemplifying the gating strategy is provided in the Supplementary Information.

Magnetic resonance imaging

Experimental design

Design type

Design specifications

Behavioral performance measures

Acquisition

Imaging type(s)

Field strength

Sequence & imaging parameters

Area of acquisition

Diffusion MRI

Used

Not used

Preprocessing

Preprocessing software

Normalization

Normalization template

Noise and artifact removal

Volume censoring

Statistical modeling & inference

Model type and settings

Effect(s) tested

Specify type of analysis: Whole brain ROI-based Both

Statistic type for inference

(See [Eklund et al. 2016](#))

Correction

Models & analysis

n/a | Involved in the study

Functional and/or effective connectivity

Graph analysis

Multivariate modeling or predictive analysis

Functional and/or effective connectivity

Graph analysis

Multivariate modeling and predictive analysis